Toward the Chemistry of Carboxylic Single-Walled Carbon Nanotubes by Chemical Force Microscopy

Yanlian Yang, Jin Zhang, Xiaolin Nan, and Zhongfan Liu*

Center for Nanoscale Science and Technology (CNST), College of Chemistry and Molecular Engineering, Peking University, Beijing 100871, P. R. China

Received: November 8, 2001; In Final Form: January 3, 2002

The present article describes the immobilization of chemically shortened single-walled carbon nanotubes (SWNTs) onto atomic force microscopy (AFM) tips using a novel wet chemistry procedure. Preliminary results on the measurement of dissociation properties of carboxylic acid groups at the open end of the shortened SWNTs in aqueous solution by chemical force microscopy (CFM) are also described. The as-prepared long SWNTs were cut into short tubes by chemical oxidation, which produced −COOH groups at the open ends of the tubes. The shortened SWNTs were covalently attached to AFM tips by surface condensation between AFM tips modified with primary amino-terminated self-assembled monolayers (SAMs) and the carboxylic groups at the exposed end of the tube. The nanotube orientation on the AFM tips was demonstrated using AFM force calibration mode. The dissociation properties of carboxylic groups at the end of SWNTs were investigated by measuring the adhesion force between SWNTs modified AFM tips and hydroxyl-terminated SAMs surfaces as a function of pH (force titration measurement). The results showed a different force titration behavior and variable p$K_{1/2}$ values between different SWNTs tips, indicating variations in the chemistry of the oxidized tubes from sample to sample. Successful attachment of carbon nanotubes to AFM tips has opened up a considerable number of possibilities in increasing the resolution of AFM procedures. Most importantly, the present investigation has provided a means of investigating the chemical properties of nanotubes attached to AFM tips.

Introduction

The use of single-walled carbon nanotubes (SWNTs), for example, in field emission displays,[1−3] nanoelectronic devices,[4−6] polymer reinforcement,[7−9] and when attached to AFM tips for high-resolution studies of biological surfaces,[10,11] is still in its infancy. Preparation, characterization, and functionalization, while important aspects of nanotube technology, are still complex and difficult. Previous studies have indicated that chemical functionalization of the open ends and the side-walls of SWNTs would play a vital role in tailoring their properties and behavior.[12]

Preparation of short usable nanotubes was achieved by Liu et al. by means of chemical oxidation.[13] Haddon et al. discovered that the nanotubes became soluble or at least suspended in aqueous solution by making derivatives of them using thionyl chloride and octadecylamine.[14] This provided the added facility of being able to both modify and study nanotube properties in solution.

Functionalizing nanotubes is, if anything, rather more difficult, for example, in assigning functional groups to the ends or side-walls of the nanotubes and properly characterizing them. Smalley et al. managed to functionalize the side-walls of carbon nanotubes using elemental fluorine yielding surface derivatives with a stoichiometry approaching C_2F.[15] Functionalizing carbon nanotubes by chemical oxidation using H_2SO_4−HNO_3, HNO_3, O_3, $KMnO_4$, OsO_4, and RuO_4 has also been reported.[13,16−21] While this mainly produces carboxylic groups at the ends or the side-walls of the tube, the results were less clear, and the degree of oxidation more difficult to predict. FTIR and XPS studies have shown that, in addition to carboxylic groups, hydroxyl and carbonyl groups are often produced by this process in the oxidation of multiwalled carbon nanotubes (MWNTs).[22,23] Other undesirable effects, such as damaging the tubular structure, were also reported.

In view of the difficulties in studying the properties of functionalized nanotubes, especially, the properties of individual nanotubes, we have attempted to develop a method of producing nanotubes as self-assembled monolayers both on substrate and atomic force microscope (AFM) tips. This would allow us to carry out the chemical studies of SWNT properties on the basis of the measurement of adhesion force between SWNTs on the AFM tip and appropriate substrates, i.e., using chemical force titration.

In our previous work we developed a wet chemical approach for producing ordered arrays of SWNTs on gold surfaces using a self-assembly technique.[24] This wet chemical method allowed us to assemble thiol-derivatized SWNTs on a gold surface with the nanotubes oriented perpendicular to the surface. To study the properties of such SWNTs we need, however, to assemble SWNTs onto the AFM cantilever tips. This would then permit us to examine the interaction between SWNT-modified AFM tips and various self-assembled monolayers (SAMs), such as OH-terminated SAMs. Two methods have been reported to do this. The first is mechanical gluing, which is straightforward but time-consuming. The second is direct growth by chemical vapor deposition, which produces SWNTs with highly controllable length, but it is difficult to avoid contamination of the tips with catalysts.[25−28]

In this paper we propose a third alternative for the attachment of SWNTs to AFM tips, which is suitable for the measurement of chemical properties of the SWNTs. We have used a wet

* Author to whom correspondence should be addressed. Tel. & Fax: 86-10-6275-7157. E-mail: lzf@chem.pku.edu.cn.

10.1021/jp0140872 CCC: $22.00
Published on Web 03/30/2002

SCHEME 1: Schematic Illustration of the Preparation of Single-Walled Carbon Nanotube AFM Tips and Measurement of Force Titration

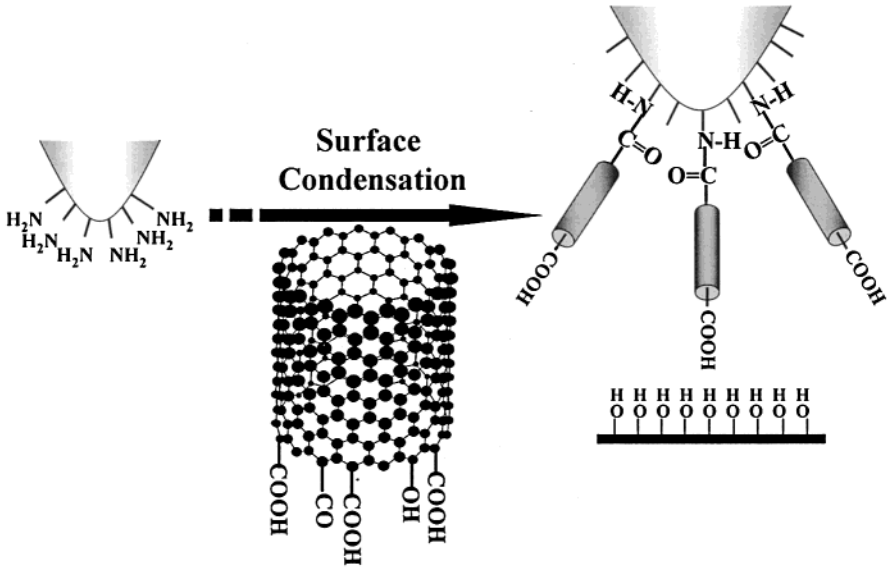

chemical approach based on condensation reactions between $-NH_2$ groups on SAMs surfaces and carboxylic groups on the SWNTs to attach the SWNTs onto AFM tips. By using this approach, the SWNTs were easily attached to the cantilever tips with the end groups exposed to the solution. The orientation of the SWNTs on the AFM tips could be demonstrated by using an AFM force calibration mode. The chemical properties of the functional groups at the open end of the SWNTs could then be examined by measuring the dissociation properties of carboxylic acid groups at the end of the nanotubes.

Experimental Section

Preparation of Shortened Single-Walled Carbon Nanotubes. The SWNTs were synthesized by a DC arc discharge method using a Y−Ni catalyst. The chemical shortening of as-prepared long nanotubes was carried out by oxidation in a mixture of concentrated sulfuric and nitric acids (3:1, 98%, and 70%, respectively) under sonication for 8 h.[13] The resulting nanotubes had typical diameters of 1.3−1.4 nm and lengths of several hundred nanometers, terminated by carboxylic groups as indicated by IR measurement.[29] The post-oxidation treatment followed the same procedure described in our previous work.[24]

AFM Tip and Substrate Preparation. The OH-terminated SAMs substrates were prepared by immersion of gold-coated silicon substrate in a 1mM ethanol solution of 11-mercaptoundecanol for 24 h. Commercial Si_3N_4 cantilever tips (Digital Instruments) were coated with 100 nm of gold by thermal evaporation onto a 10 nm adhesion layer of Ti.

Preparation of SWNTs-Modified AFM Tips. Scheme 1 illustrates the basic methodology for covalent attachment of single-walled carbon nanotubes onto AFM tips using a surface condensation reaction. The shortened nanotubes were spread in dimethylformamide (DMF, ca. 0.2 mg/mL), forming a dark-brown-colored suspension. A certain amount of dicyclohexylcarbodiimide (DCC, ca. 0.5 mg/mL) was added into the suspension and the mixture was sonicated for 10 min before use.

The $NH_2(CH_2)_{11}SH$ (AUDT, Dojindo Laboratory, Japan)-modified tips were prepared by immersing clean, gold-coated AFM tips into the AUDT ethanol solution (0.5mM) for 5 h. The AUDT molecules were found to form densely packed SAMs on the gold-coated tip.[30] The resulting AFM tip was thoroughly rinsed with ethanol and ultrapure water. After being dried in a high-purity nitrogen stream, the AFM tip was immersed in the nanotube suspension, followed by nitrogen bubbling for 5 min to remove the dissolved oxygen. The surface condensation reaction was performed at 50−60°C for ca. 12 h. All the samples were rinsed thoroughly with ultrapure water and ethanol before characterization.

Chemical Force Microscopy and Adhesion Measurements. Adhesion measurements were made with a Nanoscope E, which was equipped with a fluid cell and controlled by Nanoscope E electronics (Digital Instruments, USA). All measurements were carried out with a 10 μm × 10 μm scanner and thin, long (200 μm) Si_3N_4 cantilevers (Digital Instruments, USA) at room temperature. The adhesive interaction between SWNTs-modified tips and OH−SAMs-modified substrates was determined by recording force versus displacement curves under conditions of varying pH in a phosphate buffer ($I = 0.01$).

The force−displacement curve plots the cantilever deflection (or force when calibrated using the cantilever spring constant) versus substrate displacement. A full cycle of tip approach, contact, and retraction from the sample is recorded. The point at which the tip separates from the sample is called the pull-off point. The pull-off force at the pull-off point corresponds to the adhesion force between the tip and sample. Average adhesion force values were determined from at least 100 individual force curves at each pH value. All force versus displacement curves were captured using Nanoscope E software and later analyzed on a PC using custom software.

Results and Discussions

In our recent work,[31] we proposed a surface condensation method for the assembly of SWNTs on a gold surface. In this process the chemically shortened SWNTs are immobilized on amino-terminated SAMs on a gold surface via a condensation reaction between the amino groups and the terminal carboxylic group of the SWNTs with the aid of the condensation agent dicyclohexylcarbodiimide (DCC). Raman spectroscopy and AFM results showed that an ordered assembly of SWNTs has been formed on gold.

Direct Visualization of SWNTs on Gold Using TEM. The same methodology has now been used successfully to attach

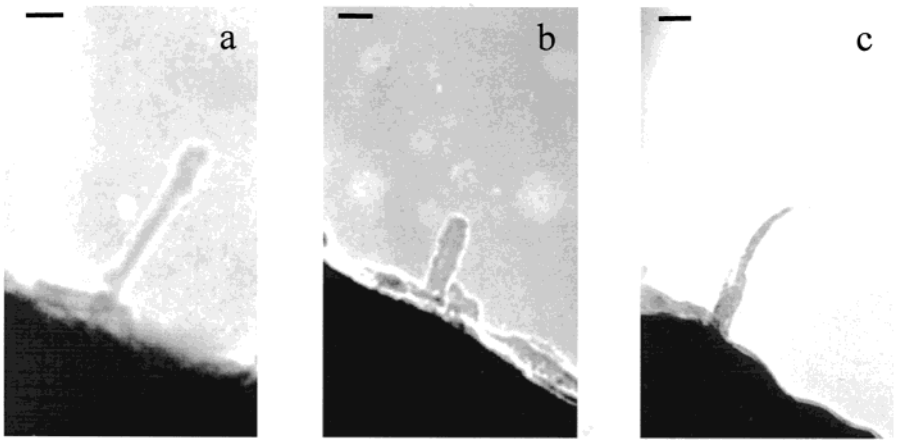

Figure 1. TEM images of the shortened SWNTs standing on gold wire surface with different tilt angles. Scale bar: (a) 10 nm, (b) 20 nm, (c) 50 nm.

the chemically shortened SWNTs to AFM tips. Direct examination of nanotubes on AFM tips is not possible with SEM because of insufficient resolution. While TEM provides sufficient resolution it is not possible to accommodate an AFM tip in a TEM sample holder. To obtain some direct visualization of the tube assemblies on gold, we have attached SWNTs to fine gold wire with the same condensation technique and imaged in the TEM. Samples for TEM observation were prepared by immersing a short length of NH_2-terminated SAMs-modified gold wire (99.99%) into the SWNTs suspension prepared by the same self-assembly process as above. The end of the gold wire was very similar to AFM tip ends. The images of the SWNTs assemblies were obtained from the edge and the end of the gold wire.

Three typical TEM images of SWNTs on gold wire surfaces are shown in Figure 1a, 1b, and 1c, respectively. The SWNTs were clearly standing more or less perpendicular to the gold surface, however, with different lengths, bundle sizes, and tilt angles. The length of the bundles ranged from 30 to 160 nm and the diameters from 2 to 22 nm. On the basis of this experiment, it is likely that SWNTs are immobilized on NH_2-terminated SAMs-modified AFM tips in very moderate conditions and will protrude more or less directly from the top of the pyramid tip with the end groups of the carbon nanotubes exposed to solution. These data suggested that the density of nanotubes or nanotube bundles immobilized on the gold wire is relatively low. Considering that the curvature radii of the gold-coated AFM tips are ca. 10 nm, it is possible that only one single nanotube or one bundle may attach to the end of the AFM tips.

Demonstration of SWNT-Modified AFM Tips. It was possible to use the chemical force microscopy (CFM) force titration technique indirectly to demonstrate the presence of SWNTs on the AFM tip. A comparison of force titration behavior between $-NH_2$-SAMs-modified AFM tip and the SWNT-modified AFM tip was carried out. The force titration behavior between the NH_2-terminated SAMs-modified AFM tip and OH-terminated SAMs modified surface is shown in the inset of Figure 2. At the lower pH, the tip would be protonated (NH_3^+) and produce lower adhesion force. As the amino groups become deprotonated with increasing pH, a larger adhesion arises presumably because of the hydrogen bond formation between $-NH_2$ groups and $-OH$ groups in agreement with previous results.[32]

After the AFM tip was modified with chemically shortened SWNTs, the force titration behavior, however, was changed completely. This behavior was similar to the behavior of a COOH-terminated tip vs OH-terminated surface (Figure 2). This

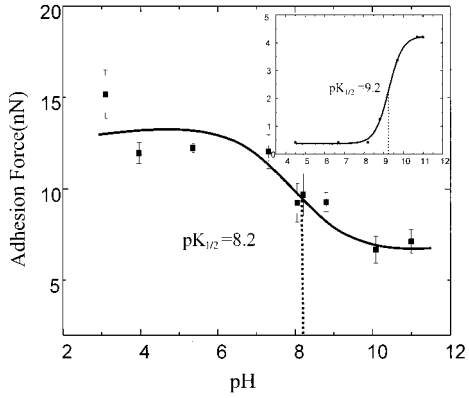

Figure 2. Force titration curve of single-walled carbon nanotube tip vs OH-terminated SAMs surface (phosphate buffer $I = 0.01$ M). The inset is the force titration curve of NH_2-terminated tips vs OH-terminated SAMs surface.

indicated that the functional groups on the AFM tip had transformed from $-NH_2$ to $-COOH$ after SWNTs modification. In other words, the tip end has transformed from $-NH_2$ to SWNTs. This also indicated that the shortened SWNTs were assembled on the AFM tips.

During the measurement of the force titration, we also found a different force calibration behavior between the traditional SAMs-modified tips or Si_3N_4 tips and SWNTs-modified AFM tips. The typical force−displacement curve of the SWNTs tip vs the OH-terminated surface (pH = 3.1, $I = 0.01$ M) was shown in Figure 3. Due to the elastically buckling behavior of the carbon nanotubes, the orientation of SWNTs on the AFM tips can be demonstrated using the AFM force calibration mode.[25,27,33] In Figure 3, two regions, A and B, were found which corresponded to the free state of the tip above the surface (region A) and the contacting state of the tip to the surface (region B). It is interesting that there is a transition in region B, which is different from the linear relationship (the inset in Figure 3) for conventional Si_3N_4 tips vs OH-terminated surface in contact region. As the tip approaches and begins to contact the sample surface, the tip jumps to contact the surface. Upon further approaching, the nanotubes begin to buckle, inducing less deflection of the cantilever (region B1), which indicated the nanotubes or bundles are oriented properly at the end of the regular tip. After the nanotubes reach their flexing limit, the cantilever deflection increases (region B2). The stiffness of the nanotube is directly related to the tube length by the relation, $F_{EULER} \propto 1/L^2$,[25] where L is the length of the nanotube. So the nanotubes we used (ca. 100 nm) are stiffer than longer (several

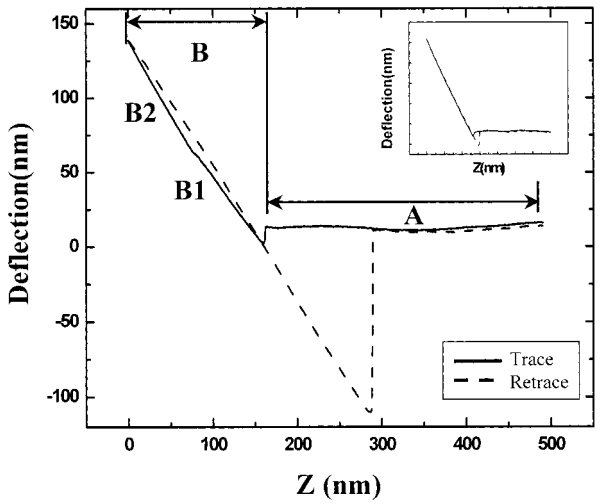

Figure 3. Typical force−displacement curve of the carbon nanotube tip vs the OH-terminated SAMs at pH = 3.1 (phosphate buffer I = 0.01 M). The inset is the force−displacement curve of a conventional Si_3N_4 tip vs an OH-terminated SAMs surface.

microns) ones. The buckling behavior lowered the deflection to a certain degree, unlike the level-off phenomenon observed in long nanotubes.[33] The stiffer short nanotube tips is more suitable for imaging varieties of surfaces than the long nanotube tips, while a little cost of deep trench resolution. During the retraction of the tip from the surface, the tip−sample adhesion, i.e., the adhesion force of functional groups on the nanotube tip vs the OH-terminated surface, can be measured from the hysteresis in the deflection plot. The force−displacement curves can be repeated many times for a given tip, indicating that the nanotubes and the covalent bonding is robust, which is an advantage for the nanotube tips used in imaging and force titration measurements.

Dissociation Properties of Carboxylic Group at the End of SWNTs. The typical chemical force titration curves of two SWNTs tips vs hydroxyl-terminated SAMs surfaces under constant ionic strength (0.01 M) phosphate buffer solutions are shown in Figure 4a and Figure 4b. The drop in adhesion force between the SWNTs tip and the OH-terminated SAMs surface with the increase of pH value is easy to explain in relation to −COOH deprotonation.

At low pH values, the carboxylic groups at the end of the SWNT tip will be fully protonated and the relatively high adhesion force can be attributed to the formation of hydrogen bonds between −COOH and −OH groups. At high pH values, when the −COOH groups are fully deprotonated, hydrogen bonds cannot form. The electrostatic repulsion between charged carboxyl and electronegative oxygen of the hydroxyl is clearly observed in the approach part of the force−distance curve (data not shown). Thus, relatively lower adhesion force can be observed.

A simple explanation for the force titration data, which initially seems reasonable, is as above. However, when considered in greater detail, there are three noticeable phenomena in the results.

First, the adhesion (ca. 7 nN) between the SWNTs tip and OH-terminated SAMs surface in Figure 4a above pH 8 is greater than that observed for traditional −COOH SAMs-modified tips, i.e., deprotonated surface, which should be zero;[34−36] while in the case of Figure 4b, the adhesion force above pH 10 similar to traditional −COOH surface is about zero. This indicates that the structures of the two different tips are different. This may be related to the presence of −CO, −OH, and −COOH groups on SWNT samples. XPS has shown these to be present in bulk samples after oxidation.[22] It seems highly probable that oxidative cutting used to prepare short SWNTs would generate −CO and/or −OH groups specifically at the cut ends of the single-walled carbon nanotubes. Hydrogen bonding between −CO, −OH groups, and −OH SAMs could well be responsible for the relatively high, i.e., above zero, adhesion force of the SWNTs tip in Figure 4a at high pH values. A near zero adhesion force in Figure 4b may indicate that −CO, −OH groups are absent on the SWNTs tip. The results support the view that the degree of oxidation is different from tip to tip.

Second, the ionic strength is seen to dramatically affect the interaction between the tip and surface. At relatively high ionic strength, taking into account the effect of the electric double layer, JKR theory gives the surface p$K_{1/2}$ at which the adhesion force is half of the way down the step between the fully protonated (maximum adhesion) and fully deprotonated (minimum adhesion) states. We can see in Figure 4 that the two different tips used thus show different p$K_{1/2}$ values (8.2 and 9.7) at the ionic strength of 0.01 M; both are, however, high relative to the −COOH SAMs.[35,36] As we know, the p$K_{1/2}$ values are affected by the ionic strength of solution and exhibit a p$K_{1/2}$ shift toward higher pH with decreasing ionic strength.[36,37] The p$K_{1/2}$ value of COOH-terminated SAMs is ca. 5.3 at 0.1 M ionic strength. The buffer used in our experiment is 0.01 M, which

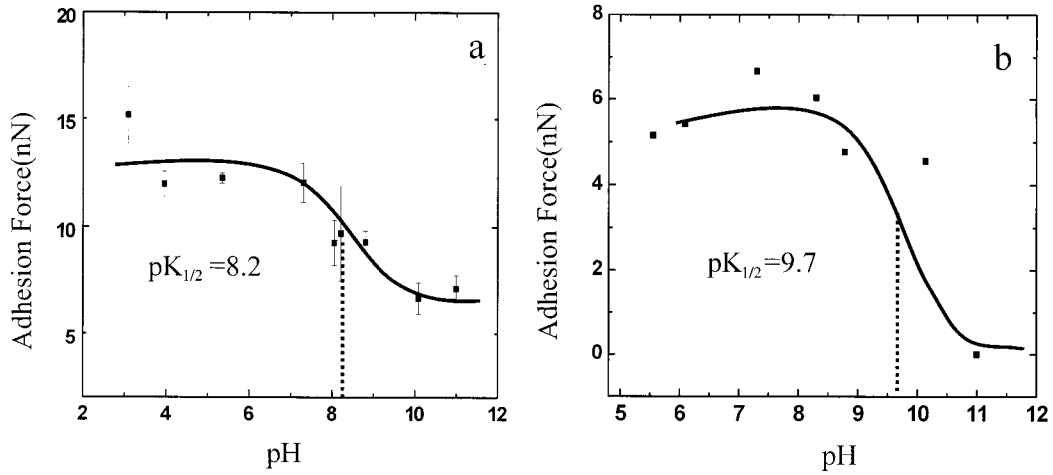

Figure 4. Two typical curves of the adhesion force of functional groups at the open end of the SWNTs immobilized on AFM tips vs OH-terminated SAMs surface (phosphate buffer I = 0.01 M).

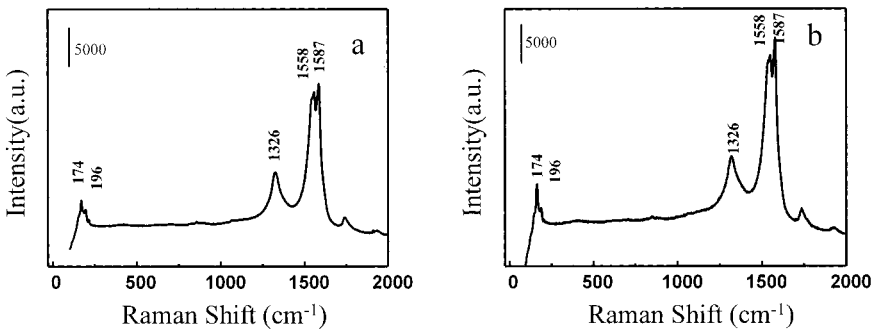

Figure 5. Raman spectra before and after force titration. (a) before, (b) after.

may introduce a p$K_{1/2}$ shift about 1.5 pH units toward higher pH, but still not enough for the results which are 2.9 and 4.4 units higher, respectively. Besides ionic strength, the p$K_{1/2}$ value of −COOH groups is determined by the degree of difficulty of −COOH ionization. In short, it is determined by the immediate chemical environment of −COOH groups at the end of the SWNTs tips. Studies have demonstrated that the carbon nanotubes, after shortening by chemical oxidation, tend to form bundles due to the attractive interactions between the hydrophobic side-walls of carbon nanotubes.[14,24] Thus the SWNTs used in these experiments, shortened by oxidation, attached to the AFM tips with our surface condensation method are likely to exhibit this hydrophobic interaction.

Finally, the additional p$K_{1/2}$ shift just indicates the complexity of the system. The p$K_{1/2}$ shift suggested a number of possibilities. According to our new high-resolution TEM results,[38] the number of SWNTs in a bundle attached to each AFM tip vary between bundles, the tilt angle of the cutting ends of the carbon nanotubes ranged in a wide region, i.e., different from one to another. The number of carboxylic groups on each tip may vary; −OH and −CO groups present on carbon nanotube tips may have an effect on the p$K_{1/2}$ values. These properties are very important for the oxidatively shortened single-walled carbon nanotubes, and further investigations are being conducted to get more information of the shortened SWNTs.

Stability of SWNTs on AFM Tips. To establish the stability of the SWNT tips, micro-Raman characterization was conducted on the pyramids of cantilever before and after the force titration of carbon nanotube tips.[39] For SWNTs, four Raman bands are strongly resonance enhanced. Three of them are located around 1600 cm^{-1}, corresponding to the characteristic A_{1g}, E_{1g}, and E_{2g} modes of graphene sheet, and the fourth strong band appears around 200 cm^{-1}, which is unique to single-walled carbon nanotubes and arises from the radial breathing mode (RBM). The typical Raman spectra of SWNTs on AFM tips are shown in Figure 5a and 5b before and after force titration measurement. From Figure 5, characteristic Raman bands of SWNTs centered around 192 cm^{-1} and 1588 cm^{-1} are clearly visible. The similarity of Raman spectra of SWNTs on AFM tips before and after the force titration indicates the satisfactory stability of the carbon nanotube tips fabricated with this surface condensation method.

In summary, we can fabricate single-walled carbon nanotube AFM tips by using a wet chemistry approach. The fabrication procedure is simple with a relatively high success rate and especially the stiff short nanotubes can be attached to the AFM tip with this novel approach. We showed the first example of investigating the chemical properties of oxidatively shortened carbon nanotubes based on force titration technique with such kinds of nanotube tips. This is demonstrated to be an effective approach to characterizing the functional groups and structures of the shortened carbon nanotubes at the tube ends. With different nanotube tips, different adhesion forces were observed at high pH values, which indicated the existence of −CO and/or −OH groups at the open ends of SWNTs and the different oxidation degree from tip to tip. The p$K_{1/2}$ values of the SWNTs may be a good indicator for their structure and chemistry.

Acknowledgment. Financial supports from the National Natural Science Foundation of China (NSFC, 6989022, 29803002, 29973001, 30000044) are gratefully acknowledged. We also thank Professor Colin Robinson, University of LEEDS, U.K., for helpful discussion.

References and Notes

(1) de Heer, W. A.; Chatelain, A.; Ugarte, D. *Science* **1995**, *270*, 1179.
(2) Choi, W. B.; Jin, Y. W.; Kim, H. Y.; et al. *Appl. Phys. Lett.* **2001**, *78*, 1547.
(3) Wang, Q. H.; Setlur, A. A.; Lauerhaas, J. M.; Dai, J. Y.; Seeling, E. W.; Chang, R. P. H. *Appl. Phys. Lett.* **1998**, *72*, 2912.
(4) Saito, S. *Science* **1997**, *278*, 77.
(5) Tans, S. J.; Verscheueren, A. R. M.; Dekker, C. *Nature* **1998**, *393*, 49.
(6) Lefebvre, J.; Antonov, R. D.; Radosavljevic, M.; et al. *Carbon* **2000**, *38*, 1745.
(7) Haggenmueller, R.; Gommans, H. H.; Rinzler, A. G.; et al. *Chem. Phys. Lett.* **2000**, *330*, 219.
(8) Jin, Z.; Pramoda, K. P.; Xu, G.; Goh, S. H. *Chem. Phys. Lett.* **2001**, *337*, 43.
(9) Ajayan, P. M.; Schadler, L. S.; Giannaris, C.; Rubio, A. *Adv. Mater.* **2000**, *12*, 750.
(10) Wong, S. S.; Harper, J. D.; Lansbury, P. T., Jr.; et al. *J. Am. Chem. Soc.* **1998**, *120*, 603.
(11) Wong, S. S.; Woolley, A. T.; Odom, T. W.; et al. *Appl. Phys. Lett.* **1998**, *73*, 3465.
(12) Edelmann, F. T. *Angew. Chem., Int. Ed.* **1999**, *38*, 1381.
(13) Liu, J.; Rinzler, A. G.; Dai, H.; Hafner, J. H.; et al. *Science* **1998**, *280*, 1253.
(14) Chen, J.; Hamon, M. A.; Hu, H.; Chen, Y.; Rao, A. M.; Eklund, P. C.; Haddon, R. C. *Science* **1998**, *282*, 95.
(15) Mickelson, E. T.; Huffman, C. B.; et al. *Chem. Phys. Lett.* **1998**, *296*, 188,
(16) Kyotani, T.; Nakazaki, S.; Xu, W.-H.; Tomita, A. *Carbon* **2001**, *39*, 782.
(17) Li, B.; Lian, Y. F.; Shi, Z. J.; Gu, Z. N. *Chem. J. Chin. Univ.* **2000**, *21*, 1633.
(18) Mawhinney, D. B.; Naumenko, V.; Kuznetsova, A.; Yates, J. T., Jr.; Liu, J.; Smalley, R. E. *Chem. Phys. Lett.* **2000**, *324*, 213.
(19) Mawhinney, D. B.; Naumenko, V.; Kuznetsova, A.; Yates, J. T., Jr.; Liu, J.; Smalley, R. E. *J. Am. Chem. Soc.* **2000**, *122*, 2383.
(20) Hernadi, K.; Siska, A.; Thien-Nga, L.; et al. *Solid State Ionics* **2001**, *141*, 203.
(21) Hwang, K. C. *J. Chem. Soc., Chem. Commun.* **1995**, *2*, 173.
(22) Hiura, H.; Ebbesen, T. W.; Tanigaki, K. *Adv. Mater.* **1995**, *7*, 275.
(23) Kuznetsova, A.; Mawhinney, D. B.; Naumenko, V.; Yates, J. T., Jr.; Liu, J.; Smalley, R. E. *Chem. Phys. Lett.* **2000**, *321*, 292.
(24) Liu, Z. F.; Shen, Z. Y.; Zhu, T.; Hou, S. F.; Ying, L. Z.; Shi, Z. J.; Gu, Z. N. *Langmuir* **2000**, *16*, 3569.
(25) Dai, H. J.; Hafner, J. H.; Rinzler, A. G.; Colbert, D. T.; Smalley, R. E. *Nature* **1996**, *384*, 147.

(26) Wong, S. S.; Joselevich, E.; Woolley, A. T.; Cheung, C. L.; Lieber, C. M. *Nature* **1998**, *394*, 52.
(27) Hafner, J. H.; Cheung, C. L.; Lieber, C. M. *Nature* **1998**, *398*, 761.
(28) Hafner, J. H.; Cheung, C. L.; Lieber, C. M. *J. Am. Chem. Soc.* **1999**, *121*, 9750.
(29) The absorption band around 1720 cm^{-1} in IR spectra indicates that the carboxylic groups exist in the oxidatively shortened SWNTs.
(30) Wallwork, M. L.; Smith, D. A.; Zhang, J.; Kirkham, J.; Robinson, C. *Langmuir* **2001**, *17*, 1126.
(31) Nan, X. L.; Gu, Z. N.; Liu, Z. F. *J. Colloid Interface Sci.* **2002**, *245*, 311.
(32) Fu, Q.; Zhang, H.; He, H. X.; et al. *Chem. J. Chin. Univ.* **2000**, *21*, 1738.
(33) Cheung, C. L.; Hafner, J. H.; Lieber, C. M. *Proc. Natl. Acad. Sci.* **2000**, *97*, 3809.
(34) Vezenov, D. V.; Noy, A.; Rozsnyai, L. F.; Lieber, C. M. *J. Am. Chem. Soc*. **1997**, *119*, 2006.
(35) He, H. X.; Huang, W.; Zhang, H.; Li, Q. G.; Li, S. F. Y.; Liu, Z. F. *Langmuir* **2000**, *16*, 517.
(36) Smith, D. A.; Wallwork, M. L.; Zhang, J.; et al. *J. Phys. Chem. B* **2000**, *104*, 8862.
(37) Zhang, J.; Kirkham, J.; Robinson, C.; et al. *Anal. Chem.* **2000**, *72*, 1973.
(38) Liu, Z. F.; et al. In preparation.
(39) Renishaw System 1000 Raman imaging System (Renishaw plc, U.K.), equipped with a 632.8 nm, 25 mW He−Ne laser (Spectra Physics, USA) and a BH-2 microscope (Olympus, Japan). The incident light was introduced to the sample through a 50× objective as a spot less than 2 μm in diameter with the power no more than 5 mW. The backscattered light from the sample was collected through the same objective. The spectrum was the average of at least 10 spectra at different spots.